

Primordial Black Hole Dark Matter and LIGO/Virgo Merger Rate
from Inflation with Running Spectral Indices:
Formation in the Matter- and/or Radiation-Dominated Universe

Kazunori Kohri^{1,2,3} and Takahiro Terada¹

¹*Theory Center, IPNS, KEK, 1-1 Oho, Tsukuba, Ibaraki 305-0801, Japan*

²*The Graduate University for Advanced Studies (SOKENDAI), 1-1, Oho, Tsukuba, Ibaraki 305-0801, Japan*

³*Rudolf Peierls Centre for Theoretical Physics, The University of Oxford, 1 Keble Road, Oxford OX1 3NP, UK*

Abstract

We study possibilities to explain the whole dark matter abundance by primordial black holes (PBHs) or to explain the merger rate of binary black holes estimated from the gravitational wave detections by LIGO/Virgo. We assume that the PBHs are originated in a radiation- or matter-dominated era from large primordial curvature perturbation generated by inflation. We take a simple model-independent approach considering inflation with large running spectral indices which are parametrized by n_s , α_s , and β_s consistent with the observational bounds. The merger rate is fitted by PBHs with masses of $\mathcal{O}(10) M_\odot$ produced in the radiation-dominated era. Then the running of running should be $\beta_s \sim 0.025$, which can be tested by future observation. On the other hand, the whole abundance of dark matter is consistent with PBHs with masses of asteroids ($\mathcal{O}(10^{-17}) M_\odot$) produced in an early matter-dominated era if a set of running parameters are properly realized.

1 Introduction

After the first detection of gravitational wave which is directly emitted from a merger of a binary black hole (BH) by LIGO/Virgo collaboration [1], interests in primordial black holes (PBHs) [2, 3] have been revived [4–10]. The masses of BHs to fit the merger rate distribute at around $\sim 30M_\odot$, where M_\odot denotes the solar mass ($= 2.0 \times 10^{33}$ g). The masses in this range are higher than those of typical binary BHs (BBHs) formed in astrophysical scenarios at the final stage of stellar evolution of main sequence stars with solar metallicity Z_\odot [11–13]. For somewhat lower metallicity $\mathcal{O}(0.1-0.01)Z_\odot$, however, such heavy BBHs can be produced [14–16]. It is also possible that BBHs with masses of $\sim 30 M_\odot$ can be formed after deaths of Population III (Pop. III) stars with their much lower metallicities [17], but there still exist large uncertainties in theoretical predictions of the merger rate, which conservatively amount to a factor of $\mathcal{O}(10^2)$ due to unknown astrophysical parameters [15, 18].

On the other hand, PBHs can be produced in the early universe through collapses of enhanced curvature perturbations¹ much before any compact stellar objects are formed. In this case, the abundance of PBHs are calculated from the curvature perturbation with less ambiguities [21, 22] once a cosmological history is fixed. Then we can potentially explain the BH merger rate inferred from the first LIGO/Virgo event, $2-53 \text{ Gpc}^{-3} \text{ yr}^{-1}$ [23], although only formation rates to produce the BBHs have some uncertainties within a couple of orders of magnitude [4–6, 24]. Because so far five BH merger events have been detected by LIGO/Virgo [1, 25–28], this motivation becomes firmer. Moreover, PBHs serve as a candidate of “non-baryonic” cold dark matter (CDM). Thus far a lot of people have discussed this possibility for a variety of mass ranges, *e.g.*, see Refs. [8, 21, 29–38] and references therein. Also, there is a scenario in which DM is produced by Hawking radiation of PBHs [39, 40]. PBHs are an interesting dark matter (DM) candidate from the particle physics perspective because we do not have to introduce new degrees of freedom beyond the Standard Model to explain DM.

In this paper, we explain the BH merger rate or the entire DM abundance by PBHs, but not both at the same time. We consider inflation with “running spectral indices”,

$$\alpha_s = \frac{\partial n_s}{\partial \ln k}, \quad \beta_s = \frac{\partial^2 n_s}{\partial (\ln k)^2}, \quad (1)$$

where k is the wave number, and n_s is the spectral index of the primordial curvature perturbation. These parameters give a quite simple phenomenological and model-independent descriptions of the power spectrum of the curvature perturbations. A large positive running, which is sometimes realized by a large “running of running” β_s , can predict a large fluctuation at small scales in

¹For other mechanisms to produce PBHs, there may exist collapses of cosmic strings, critical collapses, collapses during phase transitions, and so on (see Ref.[19, 20] and references therein).

which we are interested [41–50]. In earlier works including Refs. [37, 51–65], the BH merger rate for LIGO/Virgo events and/or the DM abundance in inflationary scenarios have been discussed. Here we do not explicitly introduce features like double inflation [58, 62] or additional fields like a curvaton [59, 61, 63] to explain DM or LIGO/Virgo events. It is remarkable and encouraging that such a simple inflationary power spectrum can account for the LIGO/Virgo BH merger rate or the whole DM. The former (latter) is explained by the PBHs of intermediate masses $M \sim \mathcal{O}(10)M_\odot$ (asteroid masses $M \sim \mathcal{O}(10^{-17})M_\odot$). Another feature of this paper is that we consider both cases of BH formation in the radiation-dominated (RD) era and in an early matter-dominated (MD) era. The latter is less extensively studied in the literature, but it is well-motivated in the inflationary cosmology since *e.g.* the coherent oscillation phase of the inflaton before reheating behaves as a MD era. For the probability of PBH formations in a MD era, we take into account the effects of anisotropies [66–68] and angular momentum [22], which suppress the PBH formation compared to the case without these effects [66, 69]. Differences of this paper from Ref. [59] include the facts that we also consider the running of running parameter β_s , that we take into account the effects of angular momentum on the PBH formation rate in the MD era, and that we do not rely on a spectator field.

In the next section, we introduce parametrization of the power spectrum of the curvature perturbations with the parameters for the running spectral indices. In Sec. 3, the probability of the PBH formation is reviewed in a RD or a MD era, and its relation to the current abundance of PBHs is introduced. Observational constraints on PBH abundance and curvature perturbations are summarized in Sec. 4. The main part of the paper is written in Sec. 5 where we scan running parameters and find allowed regions to fit either the LIGO/Virgo events or all the DM abundance. The conclusions are given in Sec. 6.

2 Inflation with running parameters

We assume that the origin of the primordial curvature perturbations needed for the PBH formation is the same as that produced by the inflaton perturbations. We take a phenomenological approach which is independent of details of inflation models. Then, we simply parametrize the primordial curvature perturbations as

$$P_\zeta(k) = A_s \left(\frac{k}{k_*} \right)^{n_s - 1 + \frac{\alpha_s}{2} \ln\left(\frac{k}{k_*}\right) + \frac{\beta_s}{6} \left(\ln\left(\frac{k}{k_*}\right) \right)^2}, \quad (2)$$

where $A_s = (2.207 \pm 0.074) \times 10^{-9}$ (Planck 2015 TT,TE,EE+lowP (68% CL)) is the overall normalization [70], $k_* = 0.05\text{Mpc}^{-1}$ is the pivot scale, n_s is the spectral index, and α_s is its running, and β_s is its running of running. The parametrization considering higher-order corrections up

to β_s is used by the Planck collaboration [71]. Thus, we can compare those parameters with observations of cosmic microwave background (CMB).

Because the scales of the wave number k which are typical for CMB observations and for productions of the PBH are different from each other, this parametrization may have limitations partly on the use of comparisons. For example, if it is the case of $\ln(k/k_*) \gg 1$, higher-order runnings could become more important. Their magnitudes depend on details of an inflaton potential or possible additional light fields like a curvaton. After emphasizing this fact, we take simplicity instead of generality. Our parameters can be directly compared with CMB, and we do not introduce additional ingredients explicitly such as double inflation or spectator fields (curvatons). For definiteness, we assume the curvature perturbations are adiabatic and Gaussian. We also assume for simplicity that inflation ends instantaneously. The last assumption would be an aggressive one for the purpose only to avoid constraints, but would be conservative when one tries to explain the dark matter abundance or the merger rate. We will briefly discuss to what extent we can relax this assumption. When the e-folding number during the inflation is small, another second inflation should follow the (first) inflation which produced perturbations.²

From the current observations, the running parameters α_s and β_s are surely consistent with zero, but can also take finite values. A negative value of α_s is favored when β_s is turned off, but this tendency no longer remains when the latter is turned on. The current constraints on these parameters due to Planck 2015 TT, TE, EE+lowP (68% CL) are as follows [71],

$$n_s = 0.9586 \pm 0.0056, \quad (3)$$

$$\alpha_s = 0.009 \pm 0.010, \quad (4)$$

$$\beta_s = 0.025 \pm 0.013. \quad (5)$$

We adopt these bounds on the parameters.³

As will be shown later, we definitely need a finite positive value of β_s to fit the LIGO/Virgo merger rate by the PBHs produced at around $k = k_{\text{LIGO}} \sim 10^6 \text{ Mpc}^{-1}$. The curvature perturbation is required to be $P_\zeta(k_{\text{LIGO}}) \sim 3 \times 10^{-2}$ at $k = k_{\text{LIGO}}$. By putting $P_\zeta(k_*) = A_s = 2.2 \times 10^{-9}$

² Typically, 50 to 60 e-foldings are required depending on the scale of inflation and the details of reheating. For example, if the e-folding number of the first inflation with the running parameters is 30, a second inflation with 20 to 30 e-foldings is implicitly assumed.

³ The Planck 2018 (TT, TE, EE+lowE+lensing) constraints [72], which were released after the completion of this paper, are

$$n_s = 0.9625 \pm 0.0048, \quad (6)$$

$$\alpha_s = 0.002 \pm 0.010, \quad (7)$$

$$\beta_s = 0.010 \pm 0.013. \quad (8)$$

The values of the parameters used in this paper are consistent with these constraints except for a small portion of Fig. 2, which in any case cannot produce a substantial amount of PBHs. In particular, the benchmark points for LIGO/Virgo (Fig. 3) and for dark matter (Fig. 6) are still well within the 2σ bound.

and $N(k_{\text{LIGO}}) \equiv \ln(k_{\text{LIGO}}/k_*) \sim 17$ into Eq. (2) with $n_s - 1 \sim -0.04$, we find a relation of the condition to produce the PBHs to be

$$-0.04 \left(\frac{n_s - 1}{-0.04} \right) \left(\frac{N(k_{\text{LIGO}})}{17} \right) + 0.1 \left(\frac{\alpha_s}{0.01} \right) \left(\frac{N(k_{\text{LIGO}})}{17} \right)^2 + 0.1 \left(\frac{\beta_s}{0.002} \right) \left(\frac{N(k_{\text{LIGO}})}{17} \right)^3 \sim 1. \quad (9)$$

For the observational constraint on the running, $|\alpha_s| \lesssim 0.01$, we approximately need a positive running of running with the order of $\beta_s \sim 0.02$. On the other hand, PBHs for dark matter require smaller values for the running parameters, as we will see in the subsequent sections.

The running parameters are constrained also by supernovae lensing [73, 74]. It involves nonlinear evolution and astrophysical uncertainties, so we do not adopt such bounds here. Nevertheless, it is easy to compare our results with such constraints.

3 PBH formation probability

The fraction of PBHs in the energy density at the time of PBH formation is conventionally denoted by β , which should not be confused with the running of running β_s . The fraction β can also be interpreted as the probability for a given Hubble patch to become a PBH. It depends on the equation of state of the universe.

3.1 PBH formation in a RD era

To consider the PBH formation, it is appropriate to smooth out subhorizon modes because it is largely determined by the horizon mass but not by tiny structures inside the horizon approximately. (For more precise computations however, we need details of the profile for the density perturbation [75, 76].) We define a coarse grained density perturbation σ [77],

$$\sigma^2(k) = \int_{-\infty}^{\infty} d \ln q w^2 \left(\frac{q}{k} \right) \frac{4(1 + w_{\text{eos}})^2}{(5 + 3w_{\text{eos}})^2} \left(\frac{q}{k} \right)^4 P_{\zeta}(q), \quad (10)$$

where $w(k) = \exp(-k^2/2)$ is a Gaussian window function, and $w_{\text{eos}} = P/\rho$ is the equation-of-state parameter ($w_{\text{eos}} = 1/3$ in the RD era; P and ρ are the pressure and the energy density). In the above expression, an weighted average is taken with respect to the wavenumber q with a smaller weight for a large $q (\gtrsim k)$ according to the window function. The transfer function of the density perturbations has been neglected because it is not important for the Gaussian window function [78]. The σ , encoding the information of the power spectrum P_{ζ} , measures the typical strength (standard deviation) of density perturbations.

In the Press-Schechter formalism [79], a PBH forms just after the density perturbation δ larger than a critical value δ_c enters the Hubble horizon. Assuming that the density perturbation

δ obeys the Gaussian distribution with the variance σ^2 , this criterion means that the PBH formation probability is given by

$$\beta(\sigma) = \int_{\delta_c}^{\infty} \frac{1}{\sqrt{2\pi}N\sigma} \exp\left(\frac{-\delta^2}{2\sigma^2}\right) d\delta \simeq \frac{1}{2} \text{Erfc}\left(\frac{\delta_c}{\sqrt{2}\sigma}\right), \quad (11)$$

where $N = \int_{-1}^{\infty} \frac{1}{\sqrt{2\pi}\sigma} \exp\frac{\delta}{2\sigma^2} d\delta$ is the normalization factor. The critical value δ_c is 1/3 in a simple analytic derivation [21] and 0.42 - 0.56 in more sophisticated approaches [75, 80–85]. We take $\delta_c = 0.42$ as a reference value in this paper. The lower end of the integral of N is set to -1 since perturbations with $\delta < -1$ is not produced. However, $\sigma \ll 1$ in our relevant parameter space, which means the integral is dominated at $|\delta| \ll 1$. Therefore, N is approximated to unity in the second equality.

To reduce the calculation cost, we approximate σ to be

$$\sigma^2(k) = \frac{2(1 + w_{\text{eos}})^2}{(5 + 3w_{\text{eos}})^2} P_{\zeta}(k), \quad (12)$$

which is exact when $P_{\zeta}(k)$ is scale invariant. Even when the running parameters are introduced, the ratio of the exact and the approximated σ^2 is roughly within an order of magnitude. This is within the same magnitude as that of uncertainties coming from the choice of the window function.

3.2 PBH formation in a MD era

In the MD era ($w_{\text{eos}} = 0$), density fluctuations grow in proportion to the scale factor once the scales of the corresponding wavelengths enter the Hubble horizon. In contrast to the RD case, initially small fluctuations can become large and eventually collapse to a PBH if the MD era is sufficiently long [66, 69]. This effect significantly enhances the formation probability of PBHs compared to the case of the RD era. However, effects of anisotropies [68] and accumulating angular momentum of the perturbed region [22] suppress the formation probability. The analytic expression is approximately given by the following formula [22],

$$\beta(\sigma) = \begin{cases} 1.894 \times 10^{-6} \times f_Q \mathcal{I}^6 \sigma^2 \exp\left(-0.1474 \frac{\mathcal{I}^{4/3}}{\sigma^{2/3}}\right) & (\sigma < 0.005) \\ 0.05556 \sigma^5 & (\sigma \geq 0.005) \end{cases} \quad (13)$$

where \mathcal{I} is a dimensionless variable characterizing the magnitude of the angular momentum of the system, Q is a dimensionless parameter measuring the initial quadrupole moment of the mass, and f_Q is the fraction of masses whose Q is below a critical value. The continuity of β leads to $f_Q \simeq 0.57$ for $\mathcal{I} = 1$. In our calculation, we use more precise numerical data to actually plot $\beta(\sigma)$ in Fig. 5 of Ref. [22] instead of the above formula.

3.3 Current PBH abundance

We consider the present value (or the value just before the PBHs evaporate) of the fraction f_{PBH} of the energy density of PBHs to that of cold dark matter (CDM), which is defined as

$$f_{\text{PBH}} = \frac{\rho_{\text{PBH}}}{\rho_{\text{CDM}}}, \quad (14)$$

where ρ_X ($X = \text{PBH}, \text{CDM}$) is the energy density of PBH or CDM. We introduce the differential energy density and fraction by

$$\rho_{\text{PBH}}(M) = \frac{d\rho_{\text{PBH}}}{d \ln(M/M_\odot)}, \quad f_{\text{PBH}}(M) = \frac{df_{\text{PBH}}}{d \ln(M/M_\odot)}, \quad (15)$$

so that the total fraction is obtained as a logarithmic integral,

$$f_{\text{PBH}} = \int d \ln(M/M_\odot) f_{\text{PBH}}(M). \quad (16)$$

The fraction $f_{\text{PBH}}(M)$ can be calculated by using the PBH formation probability $\beta(\sigma)$ introduced in the previous subsections. Then we obtain

$$f_{\text{PBH}}(M) = \left(\frac{g_*(T)}{g_*(T_{\text{eq}})} \frac{g_{*,s}(T_{\text{eq}})}{g_{*,s}(T)} \frac{T}{T_{\text{eq}}} \gamma \beta(\sigma(k(M))) \right) \Big|_{T=\text{Min}[T_M, T_R]} \frac{\Omega_m}{\Omega_{\text{CDM}}}, \quad (17)$$

where g_* ($g_{*,s}$) is the effective relativistic degrees of freedom for energy (entropy) density, T_{eq} is the temperature at the (later) matter-radiation equality, Ω_X ($X = \text{m}, \text{CDM}$) is the energy density fraction of non-relativistic matter or CDM, and we used $\gamma\beta = \frac{\rho_{\text{PBH}}(M)}{\rho_{\text{total}}(T)}$ with γ denoting the fraction of the horizon mass which actually enters the PBH. Explicitly, the definition of γ is given by the following relation

$$M = \gamma \times \frac{4\pi}{3} H^{-3} \rho. \quad (18)$$

In a RD era, a simple analytic formula $\gamma = (1/\sqrt{3})^3$ is known [21], while we set $\gamma = 1$ in a MD era. The expression inside the large parenthesis on the right-hand side of eq. (17) is evaluated at the PBH formation, which is $T = T_M$ in a RD era where T_M denotes the temperature at which the mode corresponding to the mass M enters the Hubble horizon, and $T = T_R$ (reheating temperature) dominates in the case of PBH formation in a MD era. The relation between mass M and wavenumber k is obtained by Eq. (18) supplemented with $k = aH$ and the Friedmann equation $3M_{\text{P}}^2 H^2 = \rho$ where M_{P} is the reduced Planck mass. The wavenumber is further related to the coarse-grained perturbation $\sigma(k)$ by Eq. (10).

3.4 Required amount of PBHs

Before proceeding, we summarize the requirement for the PBH abundance. The condition for the 100% dark matter abundance is simple: $f_{\text{PBH}} = 1$. The condition to explain the merger rate requires some explanation.

First, the LIGO/Virgo collaboration estimated the merger rate of BBHs as $2\text{--}53 \text{ Gpc}^{-3} \text{ yr}^{-1}$ at the 90% confidence level based on the event GW150914 [23]. It was assumed that all the BHs have the same mass and spin with those of this event.

To discuss the criterion for the merger rate, we introduce the PBH fraction $f_{\text{PBH}}^{\text{LIGO}}$ restricted to the LIGO/Virgo mass range to discuss the BH merger rate. For definiteness, we define the range as $4 \leq M/M_{\odot} \leq 40$, then

$$f_{\text{PBH}}^{\text{LIGO}} = \int_{\ln 4}^{\ln 40} d \ln(M/M_{\odot}) f_{\text{PBH}}(M). \quad (19)$$

There are largely two scenarios to produce binary systems from the PBHs. In one scenario, a BBH “forms” in the RD era when the mass of the close pair of BHs become dominant compared to the energy of surrounding radiation. This scenario requires $10^{-3} \leq f_{\text{PBH}}^{\text{LIGO}} \leq 10^{-2}$ to explain the merger rate [6]. In the other scenario, a BBH forms when two PBHs encounter with a small enough impact parameter in the late-time Universe. This mechanism is less efficient and requires $f_{\text{PBH}} \sim 1$ [4], which is in strong tension with various constraints for the $M \sim 30M_{\odot}$ mass range. Therefore, we adopt the former criterion, $10^{-3} \leq f_{\text{PBH}}^{\text{LIGO}} \leq 10^{-2}$.

Let us estimate in passing the number density of BBHs n_{BBH} in the present Universe. Using eq. (7) and the condition below eq. (3) in Ref. [6], the probability R for a close pair of BHs to form a binary is evaluated as

$$R = \frac{\int_0^{f_{\text{PBH}}^{\text{LIGO}1/3\bar{x}} dx \int_x^{\bar{x}} dy \frac{9}{\bar{x}^6} x^2 y^2}{\int_0^{\bar{x}} dx \int_x^{\bar{x}} dy \frac{9}{\bar{x}^6} x^2 y^2} = f_{\text{PBH}}^{\text{LIGO}} (2 - f_{\text{PBH}}^{\text{LIGO}}) \approx 2f_{\text{PBH}}^{\text{LIGO}}, \quad (20)$$

where x is the distance between the BHs in the binary at the time of matter-radiation equality, y is the distance of the binary to the nearest third BH, and \bar{x} is the mean separation of BHs. In the last equality, we approximated the formula assuming $f_{\text{PBH}} \ll 1$. Then n_{BBH} is estimated as

$$\begin{aligned} n_{\text{BBH}} &\simeq \frac{n_{\text{PBH}} R}{2} = 3H^2 M_{\text{P}}^2 f_{\text{PBH}}^{\text{LIGO}2} \frac{\Omega_{\text{CDM}}}{M} \\ &= 2 \times 10^2 \text{ Mpc}^{-3} \left(\frac{f_{\text{PBH}}^{\text{LIGO}}}{10^{-3}} \right)^2 \left(\frac{\Omega_{\text{CDM}} h^2}{0.12} \right) \left(\frac{M}{30M_{\odot}} \right)^{-1}. \end{aligned} \quad (21)$$

4 Observational constraints

Observational constraints on the abundance of PBHs $f_{\text{PBH}}(M)$ and the curvature fluctuations $P_\zeta(k)$ are briefly reviewed in this section. PBHs lighter than $M_{\text{evap}} = 2.6 \times 10^{-19} M_\odot$ have been evaporated by Hawking radiation [86]. The emitted radiation affects big-bang nucleosynthesis (BBN) [19], the cosmic microwave background [19, 87] and the galactic gamma-ray background [19], which in turn severely constrain the PBH abundance. PBHs slightly heavier than M_{evap} also emit energetic gamma ray, and they are constrained by the extragalactic gamma-ray background [19].

Heavier PBHs can be probed by gravitational lensing including femtolensing of gamma-ray bursts [88], microlensing constraints of Subaru/HSC [89], EROS-2 [90], and MACHO [91], and caustic crossing [92]. The constraint of Subaru/HSC turned out to be invalid for $M \lesssim 10^{-10} M_\odot$ because the geometric optics approximation is no longer valid [93–95] (see also Ref. [62]). Thus for the moment we cut the constraint below $10^{-10} M_\odot$ by hand. There are also constraints from dynamical processes such as destruction of white dwarfs by PBHs [96, 97] and absorption of neutron stars by PBHs [98]. Constraints for $10^{-5} M_\odot \lesssim M \lesssim 10^{-1} M_\odot$ could be potentially much improved, $f_{\text{PBH}} \lesssim 10^{-3} \sim 10^{-4}$, by gravitational waves from PBH-super massive BH binaries in future [99].

For larger masses ($M \gtrsim 10^2 M_\odot$), accretions of baryonic matter onto PBHs give bounds. Because baryonic matter emits high-energy photons during the accretion, reionization histories of atoms and thermal histories of the Universe are significantly modified. Then, CMB photons are affected by those high-energy photons. From observations of fluctuations and polarization for the CMB photons, the abundance of PBHs can be constrained [100, 101]. In particular, non-spherical disk-accretions occur inevitably due to a finite relative velocity between PBHs and baryonic matter. For the non-spherical nature of the accretion disks, energy deposition would be smaller, however, the reionization fraction becomes larger than the cases of spherical accretions. Then, PBHs heavier than the solar mass are severely constrained by observation [101]. Other bounds also come from radio and X-ray observations [102, 103]. Gravitational lensing of supernovae by PBHs put an independent constraint on the abundance of PBHs [104, 105]. Furthermore, PBHs are constrained by formations of large scale structure [20]. There are yet more constraints in these high mass range including survival of stars in ultra-faint dwarf galaxies (Segue I [106] and Eridanus II [107]), wide binaries [108], globular clusters [19], and so on. Not all of them are robust, but the presence of a number of independent constraints with different physical requirements indicate robustness when taken together. (However, see also Ref. [109] discussing astrophysical uncertainties for constraints on multi-solar mass PBHs.) Finally, PBHs should not exceed the total dark matter abundance, $f_{\text{PBH}} \leq 1$ [70]. These constraints on $f_{\text{PBH}}(M)$ are summarized in Ref. [19, 110] and combined in Fig. 1.

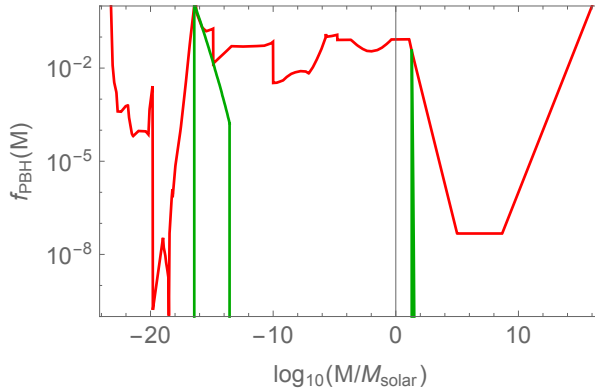


Figure 1: Constraints on the abundance of PBHs for the monochromatic mass function shown by the continuous red line. The single-peaked green lines give two independent examples of the mass function. The left one at around $10^{-16.5} - 10^{-13.5} M_{\odot}$ (from Fig. 6b) explains the whole dark matter, and the right one at around $\sim 10^1 M_{\odot}$ (from Fig. 3b) explains the BH merger rate, respectively.

To produce PBHs, large curvature perturbations are required, especially in a RD era. Such large perturbations are directly constrained by μ -distortion of CMB [111, 112] and the so-called “acoustic reheating” at BBN [113–115]. In addition, large scalar perturbations induce gravitational waves in the second order of perturbations [116, 117]. They are constrained by observations [49, 50, 118, 119], *e.g.*, through pulsar timing array (PTA) experiments [120–122].

Before closing this section, it is worth mentioning that these constraints are derived for the monochromatic mass function. For discussions on the cases with an extended mass function, see Refs. [8, 123–127]. We adopt the method in Ref. [8] to derive an appropriate constraint for our extended mass function when necessary.

5 Parameter scan results

We study the dependence of the fraction f_{PBH} of PBHs in dark matter on the parameters of the curvature perturbation with the running spectral indices. This is obtained after integrating $f_{\text{PBH}}(M)$ over the mass as in Eqs. (16) and (19).

More detailed procedure is as follows. We consider five parameters ($n_s, \alpha_s, \beta_s, T_R, H_{\text{MD}}$) where H_{MD} is the Hubble value when the early MD era begins. The end of the MD era, on the other hand, is determined by the reheating temperature T_R . For each parameter set, the wavenumber k is scanned over 18 orders of magnitude from the CMB scale to the scale corresponding to the left edge of the constraint in Fig. 1. For each k , the power spectrum $P_{\zeta}(k)$ or the mass function $f_{\text{PBH}}(M)$ is compared to the corresponding constraint. When the wavenumber

becomes larger than a critical scale⁴, the calculation of the PBH abundance assuming RD is taken over by that assuming MD. When the $P_\zeta(k)$ or $f_{\text{PBH}}(M)$ touches the constraint, we stop the scan of k (or equivalently M). This is because our power spectrum has a rising shape due to positive running parameters, and thus it will be excluded soon when k is further increased even when the constraints are for the monochromatic mass function. Then we integrate the mass function $f_{\text{PBH}}(M)$ in the relevant region. Because of the positive running in most of our parameter space, the integration is dominated by the small scale (large k , small M), and thus it is insensitive to the upper end of the integral. The results are presented below.

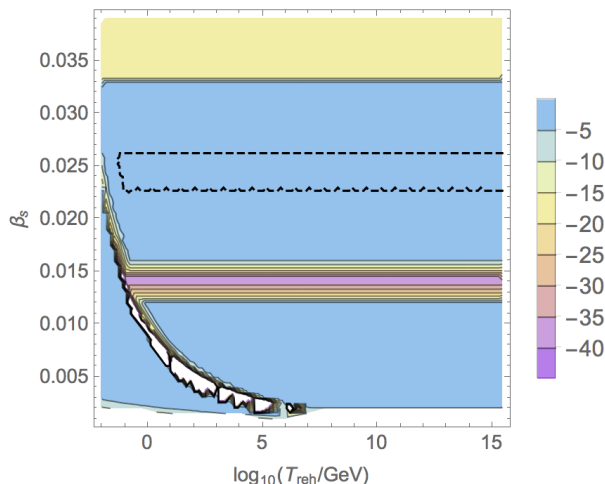


Figure 2: Contour of the logarithm of the fraction of the PBH energy density in that of dark matter, $\log_{10} f_{\text{PBH}}$. Except fine-tuned points explained below, no region can explain the whole dark matter abundance. Parameters are set as $n_s = 0.96$, $\alpha_s = 0$, and $H_{\text{MD}} = 10^{13}\text{GeV}$. The black dashed contour satisfies $f_{\text{PBH}}^{\text{LIGO}} = 10^{-3}$ and the region inside it can explain the BH merger rate implied by LIGO/Virgo gravitational wave detection. Note that the integration region of $f_{\text{PBH}}^{\text{LIGO}}$ is restricted to the LIGO/Virgo range (see Eq. (19)), while f_{PBH} does not have such a restriction (see Eq. (16)).

In Fig. 2 we show the contour of $\log_{10} f_{\text{PBH}}$ on the (β_s, T_{R}) plane. The contour of $\log_{10} f_{\text{PBH}}^{\text{LIGO}} = -3$ is also superimposed on the figure as the black dashed line. Other parameters are set to the following values: $n_s = 0.96$, $\alpha_s = 0$, and $H_{\text{MD}} = 10^{13}\text{GeV}$. Changes of n_s and α_s slightly shift the value of β_s which gives the same f_{PBH} , and a change of H_{MD} controls the maximum T_{R} but hardly affects f_{PBH} . That is why we choose the (β_s, T_{R}) plane in Fig. 2. In the figure, the upper right region is dominated by the PBHs produced in the RD era, while the lower left region is dominated by those produced in the MD era. The white band corresponds to the scale of reheating where the constraints for the RD and MD eras switch. The band and the nearby

⁴ Roughly speaking, the critical scale corresponds to the time of reheating when the early MD era ends and the RD era begins. Since the modes entering the horizon at the last stage of the MD era do not have enough time to become nonlinear, the constraint becomes weak. For such modes, we adopt the constraint for the RD era.

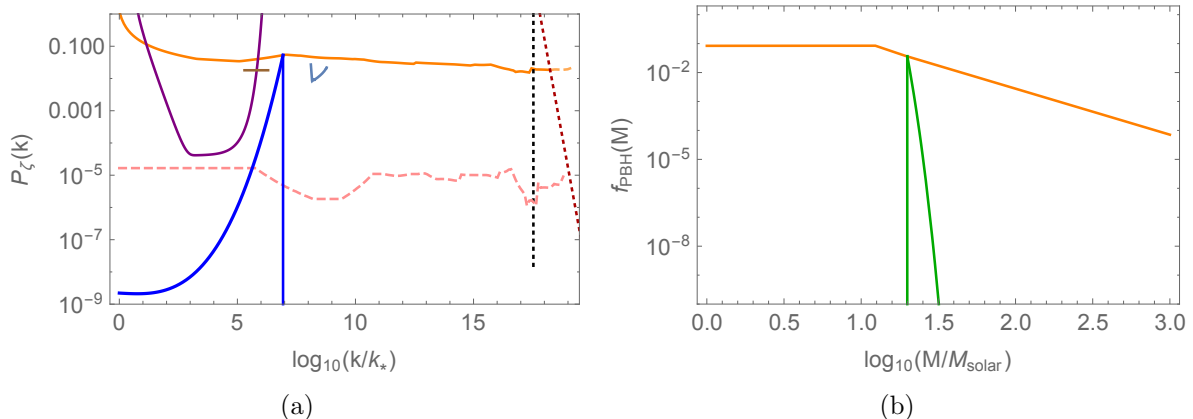


Figure 3: (a) An example of the power spectrum $P_\zeta(k)$ (blue solid line) which realizes $f_{\text{PBH}}^{\text{LIGO}} = 1.2 \times 10^{-3}$. The parameters are $n_s = 0.96$, $\alpha_s = 0$, $\beta_s = 0.026$. The orange line is the constraint on $f_{\text{PBH}}(M)$ for RD. The constraint line for MD (light red dashed line) is not effective at these scales. Other solid lines show the constraints of CMB, BBN, and PTA from left to right. The black dotted line shows the reheating at $T_R = 10^9 \text{ GeV}$, and the dark red dotted line shows the minimum k which becomes nonlinear during the MD era. (b) The corresponding mass function $f_{\text{PBH}}(M)$ (green solid line). The orange line is the constraint (for the monochromatic mass case).

non-smooth structures should not be taken seriously because this is related to the condition when we end the scan of k . The pink horizontal band near $\beta_s \simeq 0.014$ where f_{PBH} becomes tiny is due to exclusions by the PTA constraint. On the other hand, the yellow band above $\beta_s \simeq 0.33$ is due to the BBN/CMB constraint on the scalar perturbations. In these regions, the constraints are approximately independent of T_R simply because the PBH forms almost instantaneously in the RD era when the relevant mode enters the horizon, and information such as when the MD era ended is irrelevant. On the other hand, PBH formation in the MD era depends on T_R since it takes some finite time for the seed perturbations to become nonlinear.

Within the black dashed line, $10^{-3} \leq f_{\text{PBH}}^{\text{LIGO}} \leq 10^{-2}$ is satisfied, which explains [6] the BH merger rate expected from the LIGO/Virgo event, $2\text{--}53 \text{ Gpc}^{-3} \text{ yr}^{-1}$ [23]. Let us see more closely an example which realizes $10^{-3} \leq f_{\text{PBH}}^{\text{LIGO}} \leq 10^{-2}$. Fig. 3a shows the power spectrum of the primordial curvature perturbations $P_\zeta(k)$ which results in the mass function $f_{\text{PBH}}(M)$ realizing $f_{\text{PBH}}^{\text{LIGO}} = 1.2 \times 10^{-3}$ shown in Fig. 3b. For the parameter space that explains the merger rate, we have $f_{\text{PBH}}^{\text{LIGO}} \simeq f_{\text{PBH}}$ because the integral is dominated at smaller scales. This shows that in the PBH scenario for the merger rate, the dark matter abundance explained by PBHs is at most a percent level.

So far, we assumed a sharp cutoff of the curvature perturbations resulting from sudden end of inflation, which makes it easy to circumvent the PTA constraints. Let us relax this assumption and consider a milder cutoff *e.g.* by a power-law k^n . It is found in Ref. [55] that the power n

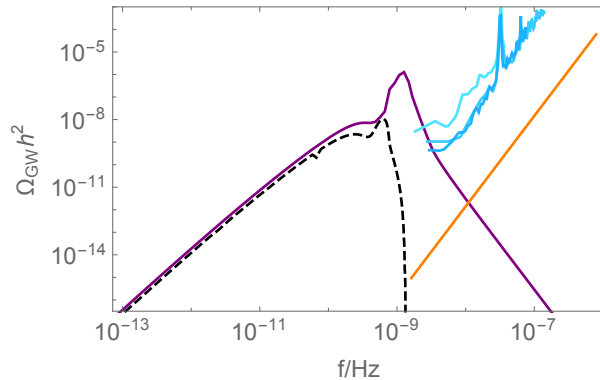


Figure 4: The gravitational wave spectrum induced by the enhanced curvature perturbations which produce PBHs explaining the LIGO/Virgo BBH merger rate (corresponding to Fig. 3). The black dashed and purple solid lines are the cases of a sharp cutoff and a power-law cutoff with the spectral index -2 , respectively. The current PTA constraints (EPTA [120], NANOGrav [122], PPTA [121]) and the future one (SKA [128]) are also shown by the bluish lines and the orange line, respectively.

must be smaller than about -2 . Although we have shown the PTA constraints on the curvature perturbation in Fig. 3a adopted from Ref. [110], it is more appropriate to calculate the induced gravitational wave spectrum and compare it with PTA constraints directly because even the monochromatic curvature perturbations induce the secondary gravitational waves with a finite width. This is done in Fig. 4 for the sharp cutoff case (black dashed line) and for the power-law case (purple solid line) using analytic formulas of Ref. [129]. We see that the power-law cutoff with the index -2 is marginally excluded by PTA experiments (bluish lines). In a realistic model, the shape of the curvature spectrum $\mathcal{P}_\zeta(k)$ will be different from ours, in particular around the peak, so it may or may not be excluded by the PTA constraints. Even so, such a spectrum will be unambiguously tested by SKA (orange line) unless the spectrum is cut off by the step function.

Next, we consider the possibility to explain dark matter by PBHs. Note that there is a small gap in the constraints on $f_{\text{PBH}}(M)$ in the asteroid-mass range $M \simeq 4 \times 10^{-17} M_\odot$. We consider parameter sets such that the corresponding mass function hits the gap where the constraint is mild in a MD era. This requires tuning of β_s for given n_s, α_s and T_R . For a higher T_R , the magnitude of $P_\zeta(k)$ required to produce a fixed $f_{\text{PBH}}(M)$ is lower. However, when T_R is too high, the asteroid mass scale is out of the MD era, and thus there is an optimum T_R around $T_R \simeq 10^4$ GeV to obtain a large f_{PBH} .

However, it is hard to find a parameter set which realizes $f_{\text{PBH}} = 1$ and does not touch the constraint at all. Remember that the constraints displayed in Fig. 1 are derived by assuming monochromatic mass functions. Therefore, we allow intersections of the mass function and the constraints, and fix the minimum PBH mass to $M = 3.69 \times 10^{-17} M_\odot$ (the high-mass boundary

of the extra-galactic gamma-ray background constraint) to enhance f_{PBH} . Instead, we adopt the prescription introduced in Ref. [8] to check whether it is really excluded. To this end, we have to calculate the integrals of $f_{\text{PBH}}(M)$ in the regions where the constraint function is a monotonically increasing or decreasing function. (These integrals to check exclusion should not be confused with the integral to obtain the total PBH fraction f_{PBH} which we always do.)

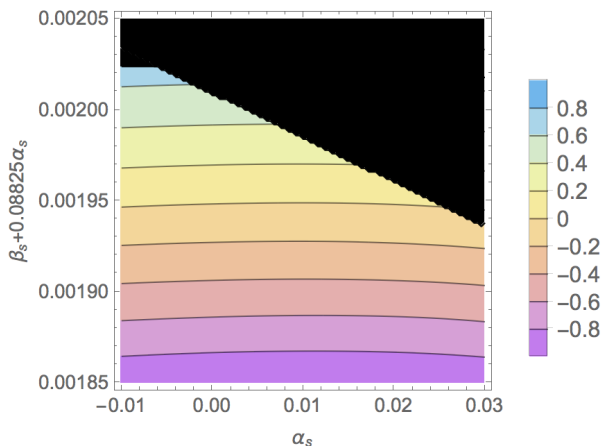


Figure 5: Contour of the logarithm of the fraction of the PBH energy density in that of dark matter, $\log_{10} f_{\text{PBH}}$, on the $(\alpha_s, \beta_s + 0.08825\alpha_s)$ plane (for visibility; the plotted region is a thin strip in the (α_s, β_s) plane). Parameters are set as $n_s = 0.96$, $T_R = 10^4 \text{ GeV}$, and $H_{\text{MD}} = 10^{13} \text{ GeV}$. The black domains are excluded by either the femto-lensing of gamma-ray burst [88] or caustic crossing [92] using the prescription for an extended mass function in Ref. [8]. In the computation, the minimum mass is taken as $3.69 \times 10^{-17} M_\odot$. See the text for details.

We find the following value of β_s results in $f_{\text{PBH}} \simeq 1$,

$$\beta_s \simeq 0.00195 - 0.08825\alpha_s, \quad (22)$$

for $n_s = 0.96$ and $T_R = 10^4 \text{ GeV}$. The contour plot of f_{PBH} on the $(\alpha_s, \beta_s + 0.08825\alpha_s)$ plane (for visibility; the plotted region is a thin strip on the (α_s, β_s) plane.) is given in Fig. 5. The black domain is excluded either by the femto-lensing of gamma-ray burst [88] or by caustic crossing [92]. The power spectrum and the mass function of an example ($\alpha_s = 0$ and $\beta_s = 0.0019485$) realizing 100% dark matter are shown in Fig. 6. Fig. 6a shows $P_\zeta(k)$ and Fig. 6b shows $f_{\text{PBH}}(M)$.

Again, the sharp cutoff assumption for the curvature perturbations is conservative for explaining the dark matter abundance, but aggressive for circumventing the constraints. We can relax the assumption and consider *e.g.* the power-law cutoff proportional to k^n . Since the slope of the constraint on $\mathcal{P}_\zeta(k)$ from the extragalactic gamma-ray background is roughly -3 , the power-law cutoff must satisfy $n \lesssim -3$. This may be hard to be realized in a concrete setup. However, in the presence of such a power-law tail, the dark matter abundance can be explained by curvature perturbations with a smaller peak, which then allows a larger power-law index.

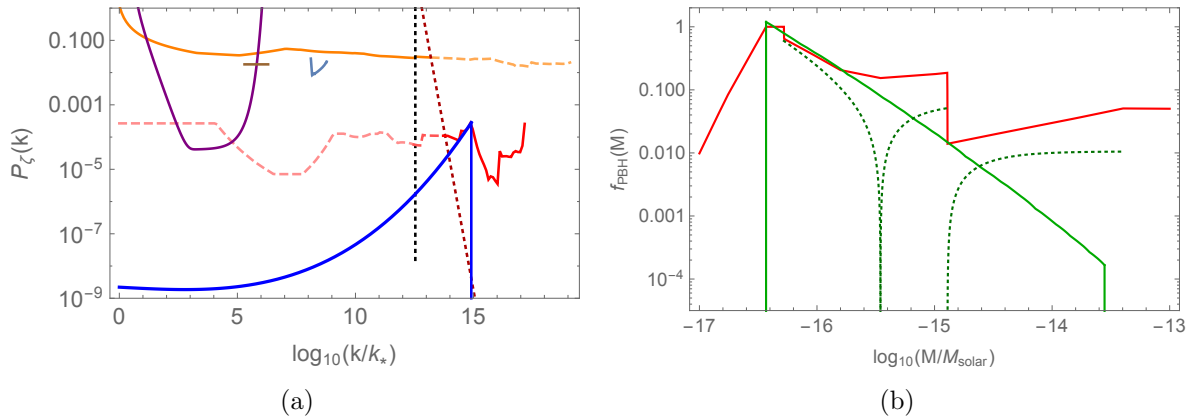


Figure 6: (a) An example of the power spectrum $P_\zeta(k)$ (blue solid line) which realizes $f_{\text{PBH}} = 1.00$. The parameters are $n_s = 0.96$, $\alpha_s = 0$, $\beta_s = 0.0019485$. The orange and red lines are the constraints on $f_{\text{PBH}}(M)$ for RD and MD respectively. Other solid lines show the constraints of CMB, BBN, and PTA from left to right. The black dotted line shows the reheating at $T_R = 10^4 \text{GeV}$, and the dark red dotted line shows the minimum k which becomes nonlinear during the MD era. (b) The corresponding mass function $f_{\text{PBH}}(M)$ (green solid line). The red line is the constraint for the monochromatic mass case. The dotted dark-green lines are integrals of $f_{\text{PBH}}(M)$ in the region where the identical constraint is monotonically increasing or decreasing. The fact that the dotted dark-green lines are always below the red line shows that this mass function is not excluded (see the text and Ref. [8] for details).

For completeness, we also show the spectra of the gravitational waves induced by the enhanced curvature perturbations in Fig. 7. We see that BBO (light green line) and DECIGO (green line) can detect the induced gravitational waves even if the spectrum is sharply cut off (black dashed line). Moreover, eLISA (cyan line) and LISA (blue line) may be able to detect them if the gravitational waves are sufficiently enhanced in the MD era (dotted lines).

6 Summary and conclusions

In this paper, we have considered the power spectrum of the curvature perturbation with running spectral indices parametrized by the parameters n_s , α_s , and β_s to produce PBHs, varying also the reheating temperature T_R which parametrizes the onset of the radiation-dominated Universe after the early matter-dominated Universe. We have shown that it is possible to explain the abundance of 100% DM or to fit the merger rate of the BBH observed from the LIGO/Virgo gravitational wave detections, utilizing the PBHs. It is notable that those fittings are possible even if we consider the serious suppression of the production rates of the PBHs due to the conservation of angular momentum for non-relativistic particles in the matter dominated Universe [22]. For the BH merger rate, we need $10^{-3} \lesssim f_{\text{PBH}}^{\text{LIGO}} \lesssim 10^{-2}$ which is obtained if $0.023 \lesssim \beta_s \lesssim 0.026$ is realized (see Fig. 2) (a precise value depends on n_s and α_s). Such a value of β_s can be probed by

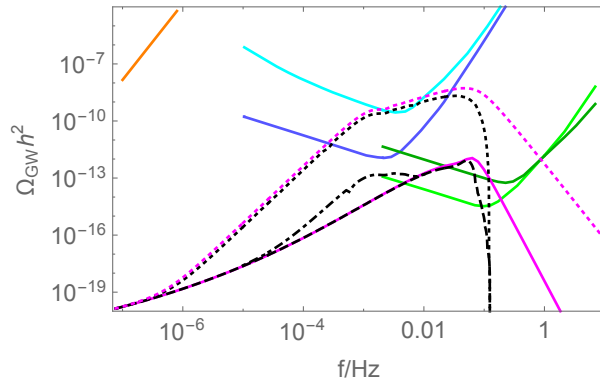


Figure 7: The gravitational wave spectrum induced by the enhanced curvature perturbations which produce PBHs explaining the dark matter abundance (corresponding to Fig. 6). The black dashed line and magenta solid line represent the standard contribution present in the radiation-dominated era for the sharp cutoff and power-law cutoff cases respectively. These are enhanced in the matter-dominated era to become the black dotted line and magenta dotted line respectively. However, these enhancements are due to extrapolation of the linear formula into the non-linear regime. The black dot-dashed line is conservative in the sense that all the contributions in the non-linear regime are neglected. For comparison, the sensitivity curves of future observations, SKA [128], eLISA [130], LISA [131], BBO [132], and DECIGO [133] are shown by the orange, cyan/blue, light green, and green lines, respectively.

future observations of the cosmological 21cm line emissions and the polarization of CMB [134]. For the 100% DM abundance, which is realized for the asteroid-mass ($\sim 10^{-17} M_{\odot}$) of PBHs, α_s and β_s have to be precisely correlated with each other for fixed n_s as shown in Eq. (22) and Fig. 5 with $T_R = 10^4$ GeV.

A lot of aspects of our work can be extended in future as our limitations are discussed in Sec. 2. It will be worth building concrete inflation models which realize characteristic features, including the running spectral indices, of the power spectrum studied in this paper. This enables us to discuss *e.g.* how quickly the running inflation ends, whether ultra slow-roll features appear [135], and how the Gaussian assumption is reasonable [136], etc. Since the power spectrum with running parameters is relatively simple, these concrete models may hopefully be simple as well.

Acknowledgments

This work is supported in part by JSPS Research Fellowship for Young Scientists (TT) and JSPS KAKENHI grant Nos. JP17J00731 (TT), JP17H01131 (KK), 26247042 (KK), and MEXT KAKENHI Grant Nos. JP15H05889 (KK), and JP16H0877 (KK).

References

- [1] **Virgo, LIGO Scientific** Collaboration, B. P. Abbott *et al.*, “Observation of Gravitational Waves from a Binary Black Hole Merger,” *Phys. Rev. Lett.* **116** no. 6, (2016) 061102, [arXiv:1602.03837 \[gr-qc\]](#).
- [2] S. Hawking, “Gravitationally collapsed objects of very low mass,” *Mon. Not. Roy. Astron. Soc.* **152** (1971) 75.
- [3] B. J. Carr and S. W. Hawking, “Black holes in the early Universe,” *Mon. Not. Roy. Astron. Soc.* **168** (1974) 399–415.
- [4] S. Bird, I. Cholis, J. B. Muñoz, Y. Ali-Haïmoud, M. Kamionkowski, E. D. Kovetz, A. Raccanelli, and A. G. Riess, “Did LIGO detect dark matter?,” *Phys. Rev. Lett.* **116** no. 20, (2016) 201301, [arXiv:1603.00464 \[astro-ph.CO\]](#).
- [5] S. Clesse and J. García-Bellido, “The clustering of massive Primordial Black Holes as Dark Matter: measuring their mass distribution with Advanced LIGO,” *Phys. Dark Univ.* **15** (2017) 142–147, [arXiv:1603.05234 \[astro-ph.CO\]](#).
- [6] M. Sasaki, T. Suyama, T. Tanaka, and S. Yokoyama, “Primordial Black Hole Scenario for the Gravitational-Wave Event GW150914,” *Phys. Rev. Lett.* **117** no. 6, (2016) 061101, [arXiv:1603.08338 \[astro-ph.CO\]](#). [erratum: *Phys. Rev. Lett.* 121, no. 5, 059901 (2018)].
- [7] Y. N. Eroshenko, “Gravitational waves from primordial black holes collisions in binary systems,” *J. Phys. Conf. Ser.* **1051** no. 1, (2018) 012010, [arXiv:1604.04932 \[astro-ph.CO\]](#).
- [8] B. Carr, F. Kuhnel, and M. Sandstad, “Primordial Black Holes as Dark Matter,” *Phys. Rev.* **D94** no. 8, (2016) 083504, [arXiv:1607.06077 \[astro-ph.CO\]](#).
- [9] J. Georg and S. Watson, “A Preferred Mass Range for Primordial Black Hole Formation and Black Holes as Dark Matter Revisited,” *JHEP* **09** (2017) 138, [arXiv:1703.04825 \[astro-ph.CO\]](#). [JHEP09,138(2017)].
- [10] M. Sasaki, T. Suyama, T. Tanaka, and S. Yokoyama, “Primordial black holes—perspectives in gravitational wave astronomy,” *Class. Quant. Grav.* **35** no. 6, (2018) 063001, [arXiv:1801.05235 \[astro-ph.CO\]](#).
- [11] K. Belczynski, T. Bulik, C. L. Fryer, A. Ruiter, J. S. Vink, and J. R. Hurley, “On The Maximum Mass of Stellar Black Holes,” *Astrophys. J.* **714** (2010) 1217–1226, [arXiv:0904.2784 \[astro-ph.SR\]](#).
- [12] M. Spera, M. Mapelli, and A. Bressan, “The mass spectrum of compact remnants from the PARSEC stellar evolution tracks,” *Mon. Not. Roy. Astron. Soc.* **451** no. 4, (2015) 4086–4103, [arXiv:1505.05201 \[astro-ph.SR\]](#).

- [13] **Virgo, LIGO Scientific** Collaboration, B. P. Abbott *et al.*, “Astrophysical Implications of the Binary Black-Hole Merger GW150914,” *Astrophys. J.* **818** no. 2, (2016) L22, [arXiv:1602.03846 \[astro-ph.HE\]](#).
- [14] K. Belczynski, M. Dominik, T. Bulik, R. O’Shaughnessy, C. Fryer, and D. E. Holz, “The effect of metallicity on the detection prospects for gravitational waves,” *The Astrophysical Journal Letters* **715** no. 2, (2010) L138. <http://stacks.iop.org/2041-8205/715/i=2/a=L138>.
- [15] K. Belczynski, D. E. Holz, T. Bulik, and R. O’Shaughnessy, “The first gravitational-wave source from the isolated evolution of two 40-100 Msun stars,” *Nature* **534** (2016) 512, [arXiv:1602.04531 \[astro-ph.HE\]](#).
- [16] K. Belczynski *et al.*, “The Effect of Pair-Instability Mass Loss on Black Hole Mergers,” *Astron. Astrophys.* **594** (2016) A97, [arXiv:1607.03116 \[astro-ph.HE\]](#).
- [17] T. Kinugawa, K. Inayoshi, K. Hotokezaka, D. Nakauchi, and T. Nakamura, “Possible Indirect Confirmation of the Existence of Pop III Massive Stars by Gravitational Wave,” *Mon. Not. Roy. Astron. Soc.* **442** no. 4, (2014) 2963–2992, [arXiv:1402.6672 \[astro-ph.HE\]](#).
- [18] T. Kinugawa, A. Miyamoto, N. Kanda, and T. Nakamura, “The detection rate of inspiral and quasi-normal modes of Population III binary black holes which can confirm or refute the general relativity in the strong gravity region,” *Mon. Not. Roy. Astron. Soc.* **456** no. 1, (2016) 1093–1114, [arXiv:1505.06962 \[astro-ph.SR\]](#).
- [19] B. J. Carr, K. Kohri, Y. Sendouda, and J. Yokoyama, “New cosmological constraints on primordial black holes,” *Phys. Rev.* **D81** (2010) 104019, [arXiv:0912.5297 \[astro-ph.CO\]](#).
- [20] B. Carr and J. Silk, “Primordial Black Holes as Generators of Cosmic Structures,” *Mon. Not. Roy. Astron. Soc.* **478** no. 3, (2018) 3756–3775, [arXiv:1801.00672 \[astro-ph.CO\]](#).
- [21] B. J. Carr, “The Primordial black hole mass spectrum,” *Astrophys. J.* **201** (1975) 1–19.
- [22] T. Harada, C.-M. Yoo, K. Kohri, and K.-I. Nakao, “Spins of primordial black holes formed in the matter-dominated phase of the Universe,” *Phys. Rev.* **D96** no. 8, (2017) 083517, [arXiv:1707.03595 \[gr-qc\]](#).
- [23] **Virgo, LIGO Scientific** Collaboration, B. P. Abbott *et al.*, “The Rate of Binary Black Hole Mergers Inferred from Advanced LIGO Observations Surrounding GW150914,” *Astrophys. J.* **833** no. 1, (2016) L1, [arXiv:1602.03842 \[astro-ph.HE\]](#).
- [24] Y. Ali-Haïmoud, E. D. Kovetz, and M. Kamionkowski, “Merger rate of primordial black-hole binaries,” *Phys. Rev.* **D96** no. 12, (2017) 123523, [arXiv:1709.06576 \[astro-ph.CO\]](#).
- [25] **Virgo, LIGO Scientific** Collaboration, B. P. Abbott *et al.*, “GW151226: Observation of Gravitational Waves from a 22-Solar-Mass Binary Black Hole Coalescence,” *Phys. Rev. Lett.* **116** no. 24, (2016) 241103, [arXiv:1606.04855 \[gr-qc\]](#).

- [26] **VIRGO, LIGO Scientific** Collaboration, B. P. Abbott *et al.*, “GW170104: Observation of a 50-Solar-Mass Binary Black Hole Coalescence at Redshift 0.2,” *Phys. Rev. Lett.* **118** no. 22, (2017) 221101, [arXiv:1706.01812 \[gr-qc\]](#). [Erratum: *Phys. Rev. Lett.*121,no.12,129901(2018)].
- [27] **Virgo, LIGO Scientific** Collaboration, B. P. Abbott *et al.*, “GW170814: A Three-Detector Observation of Gravitational Waves from a Binary Black Hole Coalescence,” *Phys. Rev. Lett.* **119** no. 14, (2017) 141101, [arXiv:1709.09660 \[gr-qc\]](#).
- [28] **Virgo, LIGO Scientific** Collaboration, B. P. Abbott *et al.*, “GW170608: Observation of a 19-solar-mass Binary Black Hole Coalescence,” *Astrophys. J.* **851** no. 2, (2017) L35, [arXiv:1711.05578 \[astro-ph.HE\]](#).
- [29] G. F. Chapline, “Cosmological effects of primordial black holes,” *Nature* **253** (1975) 251.
- [30] J. Garcia-Bellido, A. D. Linde, and D. Wands, “Density perturbations and black hole formation in hybrid inflation,” *Phys. Rev.* **D54** (1996) 6040–6058, [arXiv:astro-ph/9605094 \[astro-ph\]](#).
- [31] K. Jedamzik and J. C. Niemeyer, “Primordial black hole formation during first order phase transitions,” *Phys. Rev.* **D59** (1999) 124014, [arXiv:astro-ph/9901293 \[astro-ph\]](#).
- [32] P. H. Frampton, M. Kawasaki, F. Takahashi, and T. T. Yanagida, “Primordial Black Holes as All Dark Matter,” *JCAP* **1004** (2010) 023, [arXiv:1001.2308 \[hep-ph\]](#).
- [33] M. Kawasaki, N. Kitajima, and T. T. Yanagida, “Primordial black hole formation from an axionlike curvaton model,” *Phys. Rev.* **D87** no. 6, (2013) 063519, [arXiv:1207.2550 \[hep-ph\]](#).
- [34] K. Kohri, C.-M. Lin, and T. Matsuda, “Primordial black holes from the inflating curvaton,” *Phys. Rev.* **D87** no. 10, (2013) 103527, [arXiv:1211.2371 \[hep-ph\]](#).
- [35] P. H. Frampton, “Searching for Dark Matter Constituents with Many Solar Masses,” *Mod. Phys. Lett.* **A31** no. 16, (2016) 1650093, [arXiv:1510.00400 \[hep-ph\]](#).
- [36] G. Chapline and P. H. Frampton, “A new direction for dark matter research: intermediate mass compact halo objects,” *JCAP* **1611** no. 11, (2016) 042, [arXiv:1608.04297 \[gr-qc\]](#).
- [37] J. M. Ezquiaga, J. Garcia-Bellido, and E. Ruiz Morales, “Primordial Black Hole production in Critical Higgs Inflation,” *Phys. Lett.* **B776** (2018) 345–349, [arXiv:1705.04861 \[astro-ph.CO\]](#).
- [38] S. Clesse and J. García-Bellido, “Seven Hints for Primordial Black Hole Dark Matter,” *Phys. Dark Univ.* **22** (2018) 137–146, [arXiv:1711.10458 \[astro-ph.CO\]](#).
- [39] R. Allahverdi, J. Dent, and J. Osinski, “Nonthermal production of dark matter from primordial black holes,” *Phys. Rev.* **D97** no. 5, (2018) 055013, [arXiv:1711.10511 \[astro-ph.CO\]](#).
- [40] O. Lennon, J. March-Russell, R. Petrossian-Byrne, and H. Tillim, “Black Hole Genesis of Dark Matter,” *JCAP* **1804** no. 04, (2018) 009, [arXiv:1712.07664 \[hep-ph\]](#).

- [41] A. M. Green and A. R. Liddle, “Constraints on the density perturbation spectrum from primordial black holes,” *Phys. Rev.* **D56** (1997) 6166–6174, [arXiv:astro-ph/9704251](#) [[astro-ph](#)].
- [42] L. Covi, D. H. Lyth, and L. Roszkowski, “Observational constraints on an inflation model with a running mass,” *Phys. Rev.* **D60** (1999) 023509, [arXiv:hep-ph/9809310](#) [[hep-ph](#)].
- [43] S. M. Leach, I. J. Grivell, and A. R. Liddle, “Black hole constraints on the running mass inflation model,” *Phys. Rev.* **D62** (2000) 043516, [arXiv:astro-ph/0004296](#) [[astro-ph](#)].
- [44] K. Kohri, D. H. Lyth, and A. Melchiorri, “Black hole formation and slow-roll inflation,” *JCAP* **0804** (2008) 038, [arXiv:0711.5006](#) [[hep-ph](#)].
- [45] E. Bugaev and P. Klimai, “Constraints on amplitudes of curvature perturbations from primordial black holes,” *Phys. Rev.* **D79** (2009) 103511, [arXiv:0812.4247](#) [[astro-ph](#)].
- [46] L. Alabidi and K. Kohri, “Generating Primordial Black Holes Via Hilltop-Type Inflation Models,” *Phys. Rev.* **D80** (2009) 063511, [arXiv:0906.1398](#) [[astro-ph.CO](#)].
- [47] M. Drees and E. Erfani, “Running-Mass Inflation Model and Primordial Black Holes,” *JCAP* **1104** (2011) 005, [arXiv:1102.2340](#) [[hep-ph](#)].
- [48] M. Drees and E. Erfani, “Running Spectral Index and Formation of Primordial Black Hole in Single Field Inflation Models,” *JCAP* **1201** (2012) 035, [arXiv:1110.6052](#) [[astro-ph.CO](#)].
- [49] L. Alabidi, K. Kohri, M. Sasaki, and Y. Sendouda, “Observable Spectra of Induced Gravitational Waves from Inflation,” *JCAP* **1209** (2012) 017, [arXiv:1203.4663](#) [[astro-ph.CO](#)].
- [50] L. Alabidi, K. Kohri, M. Sasaki, and Y. Sendouda, “Observable induced gravitational waves from an early matter phase,” *JCAP* **1305** (2013) 033, [arXiv:1303.4519](#) [[astro-ph.CO](#)].
- [51] S. Clesse and J. García-Bellido, “Massive Primordial Black Holes from Hybrid Inflation as Dark Matter and the seeds of Galaxies,” *Phys. Rev.* **D92** no. 2, (2015) 023524, [arXiv:1501.07565](#) [[astro-ph.CO](#)].
- [52] S.-L. Cheng, W. Lee, and K.-W. Ng, “Production of high stellar-mass primordial black holes in trapped inflation,” *JHEP* **02** (2017) 008, [arXiv:1606.00206](#) [[astro-ph.CO](#)].
- [53] M. Kawasaki, A. Kusenko, Y. Tada, and T. T. Yanagida, “Primordial black holes as dark matter in supergravity inflation models,” *Phys. Rev.* **D94** no. 8, (2016) 083523, [arXiv:1606.07631](#) [[astro-ph.CO](#)].
- [54] J. Garcia-Bellido, M. Peloso, and C. Unal, “Gravitational waves at interferometer scales and primordial black holes in axion inflation,” *JCAP* **1612** no. 12, (2016) 031, [arXiv:1610.03763](#) [[astro-ph.CO](#)].
- [55] K. Inomata, M. Kawasaki, K. Mukaida, Y. Tada, and T. T. Yanagida, “Inflationary primordial black holes for the LIGO gravitational wave events and pulsar timing array experiments,” *Phys. Rev.* **D95** no. 12, (2017) 123510, [arXiv:1611.06130](#) [[astro-ph.CO](#)].

- [56] K. Inomata, M. Kawasaki, K. Mukaida, Y. Tada, and T. T. Yanagida, “Inflationary Primordial Black Holes as All Dark Matter,” *Phys. Rev.* **D96** no. 4, (2017) 043504, [arXiv:1701.02544](#) [[astro-ph.CO](#)].
- [57] J. Garcia-Bellido and E. Ruiz Morales, “Primordial black holes from single field models of inflation,” *Phys. Dark Univ.* **18** (2017) 47–54, [arXiv:1702.03901](#) [[astro-ph.CO](#)].
- [58] K. Kannike, L. Marzola, M. Raidal, and H. Veermäe, “Single Field Double Inflation and Primordial Black Holes,” *JCAP* **1709** no. 09, (2017) 020, [arXiv:1705.06225](#) [[astro-ph.CO](#)].
- [59] B. Carr, T. Tenkanen, and V. Vaskonen, “Primordial black holes from inflaton and spectator field perturbations in a matter-dominated era,” *Phys. Rev.* **D96** no. 6, (2017) 063507, [arXiv:1706.03746](#) [[astro-ph.CO](#)].
- [60] G. Ballesteros and M. Taoso, “Primordial black hole dark matter from single field inflation,” *Phys. Rev.* **D97** no. 2, (2018) 023501, [arXiv:1709.05565](#) [[hep-ph](#)].
- [61] K. Inomata, M. Kawasaki, K. Mukaida, Y. Tada, and T. T. Yanagida, “ $\mathcal{O}(10)M_{\odot}$ primordial black holes and string axion dark matter,” *Phys. Rev.* **D96** no. 12, (2017) 123527, [arXiv:1709.07865](#) [[astro-ph.CO](#)].
- [62] K. Inomata, M. Kawasaki, K. Mukaida, and T. T. Yanagida, “Double inflation as a single origin of primordial black holes for all dark matter and LIGO observations,” *Phys. Rev.* **D97** no. 4, (2018) 043514, [arXiv:1711.06129](#) [[astro-ph.CO](#)].
- [63] K. Ando, K. Inomata, M. Kawasaki, K. Mukaida, and T. T. Yanagida, “Primordial black holes for the LIGO events in the axionlike curvaton model,” *Phys. Rev.* **D97** no. 12, (2018) 123512, [arXiv:1711.08956](#) [[astro-ph.CO](#)].
- [64] M. P. Hertzberg and M. Yamada, “Primordial Black Holes from Polynomial Potentials in Single Field Inflation,” *Phys. Rev.* **D97** no. 8, (2018) 083509, [arXiv:1712.09750](#) [[astro-ph.CO](#)].
- [65] S.-L. Cheng, W. Lee, and K.-W. Ng, “Primordial black holes and associated gravitational waves in axion monodromy inflation,” *JCAP* **1807** no. 07, (2018) 001, [arXiv:1801.09050](#) [[astro-ph.CO](#)].
- [66] M. Yu. Khlopov and A. G. Polnarev, “PRIMORDIAL BLACK HOLES AS A COSMOLOGICAL TEST OF GRAND UNIFICATION,” *Phys. Lett.* **97B** (1980) 383–387.
- [67] M. Yu. Khlopov and A. G. Polnarev *Astron. Zh.* **59** (1982) 639. [*Sov. Astron.* **26** (1982) 391].
- [68] T. Harada, C.-M. Yoo, K. Kohri, K.-i. Nakao, and S. Jhingan, “Primordial black hole formation in the matter-dominated phase of the Universe,” *Astrophys. J.* **833** no. 1, (2016) 61, [arXiv:1609.01588](#) [[astro-ph.CO](#)].
- [69] A. G. Polnarev and M. Yu. Khlopov, “COSMOLOGY, PRIMORDIAL BLACK HOLES, AND SUPERMASSIVE PARTICLES,” *Sov. Phys. Usp.* **28** (1985) 213–232. [*Usp. Fiz. Nauk*145,369(1985)].

- [70] **Planck** Collaboration, P. A. R. Ade *et al.*, “Planck 2015 results. XIII. Cosmological parameters,” *Astron. Astrophys.* **594** (2016) A13, [arXiv:1502.01589 \[astro-ph.CO\]](#).
- [71] **Planck** Collaboration, P. A. R. Ade *et al.*, “Planck 2015 results. XX. Constraints on inflation,” *Astron. Astrophys.* **594** (2016) A20, [arXiv:1502.02114 \[astro-ph.CO\]](#).
- [72] **Planck** Collaboration, Y. Akrami *et al.*, “Planck 2018 results. X. Constraints on inflation,” [arXiv:1807.06211 \[astro-ph.CO\]](#).
- [73] I. Ben-Dayan and T. Kalaydzhyan, “Constraining the primordial power spectrum from SNIa lensing dispersion,” *Phys. Rev.* **D90** no. 8, (2014) 083509, [arXiv:1309.4771 \[astro-ph.CO\]](#).
- [74] I. Ben-Dayan and R. Takahashi, “Constraints on small-scale cosmological fluctuations from SNe lensing dispersion,” *Mon. Not. Roy. Astron. Soc.* **455** no. 1, (2016) 552–562, [arXiv:1504.07273 \[astro-ph.CO\]](#).
- [75] T. Nakama, T. Harada, A. G. Polnarev, and J. Yokoyama, “Identifying the most crucial parameters of the initial curvature profile for primordial black hole formation,” *JCAP* **1401** (2014) 037, [arXiv:1310.3007 \[gr-qc\]](#).
- [76] T. Nakama, T. Harada, A. G. Polnarev, and J. Yokoyama, “Investigating formation condition of primordial black holes for generalized initial perturbation profiles,” in *Proceedings, 10th International Symposium on Cosmology and Particle Astrophysics (CosPA 2013): Honolulu, Hawaii, USA, November 12-15, 2013*. 2014. [arXiv:1401.7740 \[gr-qc\]](#).
<http://www.slac.stanford.edu/econf/C131112/papers/1401.7740.pdf>.
- [77] S. Young, C. T. Byrnes, and M. Sasaki, “Calculating the mass fraction of primordial black holes,” *JCAP* **1407** (2014) 045, [arXiv:1405.7023 \[gr-qc\]](#).
- [78] K. Ando, K. Inomata, and M. Kawasaki, “Primordial black holes and uncertainties in the choice of the window function,” *Phys. Rev.* **D97** no. 10, (2018) 103528, [arXiv:1802.06393 \[astro-ph.CO\]](#).
- [79] W. H. Press and P. Schechter, “Formation of galaxies and clusters of galaxies by selfsimilar gravitational condensation,” *Astrophys. J.* **187** (1974) 425–438.
- [80] M. Shibata and M. Sasaki, “Black hole formation in the Friedmann universe: Formulation and computation in numerical relativity,” *Phys. Rev.* **D60** (1999) 084002, [arXiv:gr-qc/9905064 \[gr-qc\]](#).
- [81] I. Musco, J. C. Miller, and L. Rezzolla, “Computations of primordial black hole formation,” *Class. Quant. Grav.* **22** (2005) 1405–1424, [arXiv:gr-qc/0412063 \[gr-qc\]](#).
- [82] A. G. Polnarev and I. Musco, “Curvature profiles as initial conditions for primordial black hole formation,” *Class. Quant. Grav.* **24** (2007) 1405–1432, [arXiv:gr-qc/0605122 \[gr-qc\]](#).

- [83] I. Musco, J. C. Miller, and A. G. Polnarev, “Primordial black hole formation in the radiative era: Investigation of the critical nature of the collapse,” *Class. Quant. Grav.* **26** (2009) 235001, [arXiv:0811.1452 \[gr-qc\]](#).
- [84] I. Musco and J. C. Miller, “Primordial black hole formation in the early universe: critical behaviour and self-similarity,” *Class. Quant. Grav.* **30** (2013) 145009, [arXiv:1201.2379 \[gr-qc\]](#).
- [85] T. Harada, C.-M. Yoo, T. Nakama, and Y. Koga, “Cosmological long-wavelength solutions and primordial black hole formation,” *Phys. Rev.* **D91** no. 8, (2015) 084057, [arXiv:1503.03934 \[gr-qc\]](#).
- [86] S. W. Hawking, “Particle Creation by Black Holes,” *Commun. Math. Phys.* **43** (1975) 199–220. [,167(1975)].
- [87] P. Stöcker, M. Krämer, J. Lesgourgues, and V. Poulin, “Exotic energy injection with ExoCLASS: Application to the Higgs portal model and evaporating black holes,” *JCAP* **1803** no. 03, (2018) 018, [arXiv:1801.01871 \[astro-ph.CO\]](#).
- [88] A. Barnacka, J. F. Glicenstein, and R. Moderski, “New constraints on primordial black holes abundance from femtolensing of gamma-ray bursts,” *Phys. Rev.* **D86** (2012) 043001, [arXiv:1204.2056 \[astro-ph.CO\]](#).
- [89] H. Niikura *et al.*, “Microlensing constraints on primordial black holes with the Subaru/HSC Andromeda observation,” [arXiv:1701.02151 \[astro-ph.CO\]](#).
- [90] **EROS-2** Collaboration, P. Tisserand *et al.*, “Limits on the Macho Content of the Galactic Halo from the EROS-2 Survey of the Magellanic Clouds,” *Astron. Astrophys.* **469** (2007) 387–404, [arXiv:astro-ph/0607207 \[astro-ph\]](#).
- [91] **Macho** Collaboration, R. A. Allsman *et al.*, “MACHO project limits on black hole dark matter in the 1-30 solar mass range,” *Astrophys. J.* **550** (2001) L169, [arXiv:astro-ph/0011506 \[astro-ph\]](#).
- [92] M. Oguri, J. M. Diego, N. Kaiser, P. L. Kelly, and T. Broadhurst, “Understanding caustic crossings in giant arcs: characteristic scales, event rates, and constraints on compact dark matter,” *Phys. Rev.* **D97** no. 2, (2018) 023518, [arXiv:1710.00148 \[astro-ph.CO\]](#).
- [93] M. Takada, “Microlensing constraints on primordial black holes with the Subaru/HSC Andromeda observation,” 2017. Talk at Kavli IPMU in the Focus week on primordial black holes.
- [94] T. T. Nakamura, “Gravitational lensing of gravitational waves from inspiraling binaries by a point mass lens,” *Phys. Rev. Lett.* **80** (1998) 1138–1141.
- [95] R. Takahashi and T. Nakamura, “Wave effects in gravitational lensing of gravitational waves from chirping binaries,” *Astrophys. J.* **595** (2003) 1039–1051, [arXiv:astro-ph/0305055 \[astro-ph\]](#).

- [96] F. Capela, M. Pshirkov, and P. Tinyakov, “Constraints on Primordial Black Holes as Dark Matter Candidates from Star Formation,” *Phys. Rev.* **D87** no. 2, (2013) 023507, [arXiv:1209.6021](#) [[astro-ph.CO](#)].
- [97] P. W. Graham, S. Rajendran, and J. Varela, “Dark Matter Triggers of Supernovae,” *Phys. Rev.* **D92** no. 6, (2015) 063007, [arXiv:1505.04444](#) [[hep-ph](#)].
- [98] F. Capela, M. Pshirkov, and P. Tinyakov, “Constraints on primordial black holes as dark matter candidates from capture by neutron stars,” *Phys. Rev.* **D87** no. 12, (2013) 123524, [arXiv:1301.4984](#) [[astro-ph.CO](#)].
- [99] H.-K. Guo, J. Shu, and Y. Zhao, “Using LISA-like Gravitational Wave Detectors to Search for Primordial Black Holes,” [arXiv:1709.03500](#) [[astro-ph.CO](#)].
- [100] Y. Ali-Haïmoud and M. Kamionkowski, “Cosmic microwave background limits on accreting primordial black holes,” *Phys. Rev.* **D95** no. 4, (2017) 043534, [arXiv:1612.05644](#) [[astro-ph.CO](#)].
- [101] V. Poulin, P. D. Serpico, F. Calore, S. Clesse, and K. Kohri, “CMB bounds on disk-accreting massive primordial black holes,” *Phys. Rev.* **D96** no. 8, (2017) 083524, [arXiv:1707.04206](#) [[astro-ph.CO](#)].
- [102] D. Gaggero, G. Bertone, F. Calore, R. M. T. Connors, M. Lovell, S. Markoff, and E. Storm, “Searching for Primordial Black Holes in the radio and X-ray sky,” *Phys. Rev. Lett.* **118** no. 24, (2017) 241101, [arXiv:1612.00457](#) [[astro-ph.HE](#)].
- [103] Y. Inoue and A. Kusenko, “New X-ray bound on density of primordial black holes,” *JCAP* **1710** no. 10, (2017) 034, [arXiv:1705.00791](#) [[astro-ph.CO](#)].
- [104] M. Zumalacarregui and U. Seljak, “Limits on stellar-mass compact objects as dark matter from gravitational lensing of type Ia supernovae,” *Phys. Rev. Lett.* **121** no. 14, (2018) 141101, [arXiv:1712.02240](#) [[astro-ph.CO](#)].
- [105] J. Garcia-Bellido, S. Clesse, and P. Fleury, “Primordial black holes survive SN lensing constraints,” *Phys. Dark Univ.* **20** (2018) 95–100, [arXiv:1712.06574](#) [[astro-ph.CO](#)].
- [106] S. M. Koushiappas and A. Loeb, “Dynamics of Dwarf Galaxies Disfavor Stellar-Mass Black Holes as Dark Matter,” *Phys. Rev. Lett.* **119** no. 4, (2017) 041102, [arXiv:1704.01668](#) [[astro-ph.GA](#)].
- [107] T. D. Brandt, “Constraints on MACHO Dark Matter from Compact Stellar Systems in Ultra-Faint Dwarf Galaxies,” *Astrophys. J.* **824** no. 2, (2016) L31, [arXiv:1605.03665](#) [[astro-ph.GA](#)].
- [108] M. A. Monroy-Rodríguez and C. Allen, “The end of the MACHO era- revisited: new limits on MACHO masses from halo wide binaries,” *Astrophys. J.* **790** no. 2, (2014) 159, [arXiv:1406.5169](#) [[astro-ph.GA](#)].

- [109] A. M. Green, “Astrophysical uncertainties on stellar microlensing constraints on multi-Solar mass primordial black hole dark matter,” *Phys. Rev.* **D96** no. 4, (2017) 043020, [arXiv:1705.10818](#) [[astro-ph.CO](#)].
- [110] B. J. Carr, K. Kohri, Y. Sendouda, and J. Yokoyama in preparation., 2018.
- [111] J. Chluba, A. L. Erickcek, and I. Ben-Dayan, “Probing the inflaton: Small-scale power spectrum constraints from measurements of the CMB energy spectrum,” *Astrophys. J.* **758** (2012) 76, [arXiv:1203.2681](#) [[astro-ph.CO](#)].
- [112] K. Kohri, T. Nakama, and T. Suyama, “Testing scenarios of primordial black holes being the seeds of supermassive black holes by ultracompact minihalos and CMB μ -distortions,” *Phys. Rev.* **D90** no. 8, (2014) 083514, [arXiv:1405.5999](#) [[astro-ph.CO](#)].
- [113] D. Jeong, J. Pradler, J. Chluba, and M. Kamionkowski, “Silk damping at a redshift of a billion: a new limit on small-scale adiabatic perturbations,” *Phys. Rev. Lett.* **113** (2014) 061301, [arXiv:1403.3697](#) [[astro-ph.CO](#)].
- [114] T. Nakama, T. Suyama, and J. Yokoyama, “Reheating the Universe Once More: The Dissipation of Acoustic Waves as a Novel Probe of Primordial Inhomogeneities on Even Smaller Scales,” *Phys. Rev. Lett.* **113** (2014) 061302, [arXiv:1403.5407](#) [[astro-ph.CO](#)].
- [115] K. Inomata, M. Kawasaki, and Y. Tada, “Revisiting constraints on small scale perturbations from big-bang nucleosynthesis,” *Phys. Rev.* **D94** no. 4, (2016) 043527, [arXiv:1605.04646](#) [[astro-ph.CO](#)].
- [116] K. N. Ananda, C. Clarkson, and D. Wands, “The Cosmological gravitational wave background from primordial density perturbations,” *Phys. Rev.* **D75** (2007) 123518, [arXiv:gr-qc/0612013](#) [[gr-qc](#)].
- [117] D. Baumann, P. J. Steinhardt, K. Takahashi, and K. Ichiki, “Gravitational Wave Spectrum Induced by Primordial Scalar Perturbations,” *Phys. Rev.* **D76** (2007) 084019, [arXiv:hep-th/0703290](#) [[hep-th](#)].
- [118] R. Saito and J. Yokoyama, “Gravitational wave background as a probe of the primordial black hole abundance,” *Phys. Rev. Lett.* **102** (2009) 161101, [arXiv:0812.4339](#) [[astro-ph](#)]. [Erratum: *Phys. Rev. Lett.*107,069901(2011)].
- [119] R. Saito and J. Yokoyama, “Gravitational-Wave Constraints on the Abundance of Primordial Black Holes,” *Prog. Theor. Phys.* **123** (2010) 867–886, [arXiv:0912.5317](#) [[astro-ph.CO](#)]. [Erratum: *Prog. Theor. Phys.*126,351(2011)].
- [120] L. Lentati *et al.*, “European Pulsar Timing Array Limits On An Isotropic Stochastic Gravitational-Wave Background,” *Mon. Not. Roy. Astron. Soc.* **453** no. 3, (2015) 2576–2598, [arXiv:1504.03692](#) [[astro-ph.CO](#)].

- [121] R. M. Shannon *et al.*, “Gravitational waves from binary supermassive black holes missing in pulsar observations,” *Science* **349** no. 6255, (2015) 1522–1525, [arXiv:1509.07320](#) [[astro-ph.CO](#)].
- [122] **NANOGrav** Collaboration, Z. Arzoumanian *et al.*, “The NANOGrav 11-year Data Set: Pulsar-timing Constraints On The Stochastic Gravitational-wave Background,” *Astrophys. J.* **859** no. 1, (2018) 47, [arXiv:1801.02617](#) [[astro-ph.HE](#)].
- [123] A. M. Green, “Microlensing and dynamical constraints on primordial black hole dark matter with an extended mass function,” *Phys. Rev.* **D94** no. 6, (2016) 063530, [arXiv:1609.01143](#) [[astro-ph.CO](#)].
- [124] F. Kühnel and K. Freese, “Constraints on Primordial Black Holes with Extended Mass Functions,” *Phys. Rev.* **D95** no. 8, (2017) 083508, [arXiv:1701.07223](#) [[astro-ph.CO](#)].
- [125] B. Carr, M. Raidal, T. Tenkanen, V. Vaskonen, and H. Veermäe, “Primordial black hole constraints for extended mass functions,” *Phys. Rev.* **D96** no. 2, (2017) 023514, [arXiv:1705.05567](#) [[astro-ph.CO](#)].
- [126] N. Bellomo, J. L. Bernal, A. Raccanelli, and L. Verde, “Primordial Black Holes as Dark Matter: Converting Constraints from Monochromatic to Extended Mass Distributions,” *JCAP* **1801** no. 01, (2018) 004, [arXiv:1709.07467](#) [[astro-ph.CO](#)].
- [127] B. V. Lehmann, S. Profumo, and J. Yant, “The Maximal-Density Mass Function for Primordial Black Hole Dark Matter,” *JCAP* **1804** no. 04, (2018) 007, [arXiv:1801.00808](#) [[astro-ph.CO](#)].
- [128] P. E. Dewdney, P. J. Hall, R. T. Schilizzi, and T. J. L. W. Lazio, “The square kilometre array,” *Proceedings of the IEEE* **97** no. 8, (Aug, 2009) 1482–1496.
- [129] K. Kohri and T. Terada, “Semianalytic calculation of gravitational wave spectrum nonlinearly induced from primordial curvature perturbations,” *Phys. Rev.* **D97** no. 12, (2018) 123532, [arXiv:1804.08577](#) [[gr-qc](#)].
- [130] **eLISA** Collaboration, P. A. Seoane *et al.*, “The Gravitational Universe,” [arXiv:1305.5720](#) [[astro-ph.CO](#)].
- [131] P. Amaro-Seoane *et al.*, “Laser Interferometer Space Antenna,” *ArXiv e-prints* (Feb., 2017) , [arXiv:1702.00786](#) [[astro-ph.IM](#)].
- [132] G. M. Harry, P. Fritschel, D. A. Shaddock, W. Folkner, and E. S. Phinney, “Laser interferometry for the big bang observer,” *Class. Quant. Grav.* **23** (2006) 4887–4894. [Erratum: *Class. Quant. Grav.* **23**, 7361(2006)].
- [133] N. Seto, S. Kawamura, and T. Nakamura, “Possibility of direct measurement of the acceleration of the universe using 0.1-Hz band laser interferometer gravitational wave antenna in space,” *Phys. Rev. Lett.* **87** (2001) 221103, [arXiv:astro-ph/0108011](#) [[astro-ph](#)].
- [134] K. Kohri, Y. Oyama, T. Sekiguchi, and T. Takahashi, “Precise Measurements of Primordial Power Spectrum with 21 cm Fluctuations,” *JCAP* **1310** (2013) 065, [arXiv:1303.1688](#) [[astro-ph.CO](#)].

- [135] H. Motohashi and W. Hu, “Primordial Black Holes and Slow-Roll Violation,” *Phys. Rev.* **D96** no. 6, (2017) 063503, [arXiv:1706.06784 \[astro-ph.CO\]](#).
- [136] G. Franciolini, A. Kehagias, S. Matarrese, and A. Riotto, “Primordial Black Holes from Inflation and non-Gaussianity,” *JCAP* **1803** no. 03, (2018) 016, [arXiv:1801.09415 \[astro-ph.CO\]](#).